Energy and AI 6 (2021) 100102

Contents lists available at ScienceDirect

Energy and AI

journal homepage: www.sciencedirect.com/journal/energy-and-ai

Thermodynamic and kinetics of hydrogen photoproduction enhancement by concentrated sunlight with CO_2 photoreduction by heterojunction photocatalysts

Ziyu Liu [*,a,b], Teng Yi [c], Chenxu Huang [d], Kwang-Leong Choy [b], Chaozong Liu [b]

[a] School of Medical Science and Engineering, Beihang University, China
[b] Centre for Materials Research, University College London, UK
[c] National Institude of Defense Science and Technology, China
[d] Northwest Institute of Mechanical & Electrical Engineering, China

HIGHLIGHTS

- The thermodynamic and kinetic mechanism of concentrated sunlight photocatalytic system
- Photocatalytic activities related with favourable formation of p-n junctions;
- Appropriate semiconductor pairs Fe_2O_3/TiO_2 for CO_2 photoreduction and H_2 photoproduction

GRAPHICAL ABSTRACT

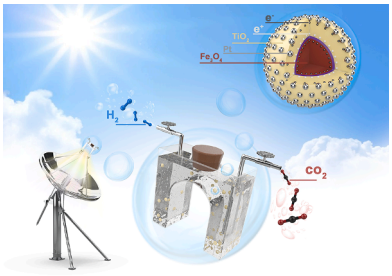

ARTICLE INFO

Keywords:
Concentrated sunlight
Hydrogen evolution
CO_2 photoreduction
p-n junction
Thermodynamics and kinetics

ABSTRACT

For achieving water splitting into hydrogen under sunlight for practical applications, the high efficiencies of the photoreduction of CO_2 over TiO_2/Fe_3O_4 photocatalysts combined with hydrogenation of water splitting over Pt/TiO_2 were investigated by practical concentrated solar energy compared with Hg lamp and Xe lamp. Based on AI analysis on the influence factors, the key parameters for TOC concentration were photocatalysts, Na_2CO_3 concentration and radiation intensity while the key parameters for hydrogen production were photocatalysts, radiation intensity, and TOC concentration. Accordingly, the mechanism of concentrated sunlight effects has been discussed from the view of thermodynamics and kinetics. The concentrated sunlight provides a simultaneous supply of sufficient electron–hole pairs and thermal energy. Water to hydrogen and CO_2 reduction are both enhanced in concentrated sunlight due to endothermal reactions. Doping changes the internal electric field of p-n junction of in different possible ways, and thus composite photocatalysts with favorable formation of p-n junctions would enhance the charge separation by internal electric field. Moreover, photocatalysts are beneficial for providing more excited electrons at a time for achieving CO_2 photoreduction at the surface region of the particles with higher density of radiation by concentrated solar energy. Subsequently, products from CO_2 photoreduction, acting as sacrificial electron donors, improved hydrogen evolution in solar-mediated water splitting for prohibiting reverse reactions.

* Corresponding author at: School of Medical Science and Engineering, Beihang University, Beijing, Beijing, China.
E-mail address: liu_ziyu@buaa.edu.cn (Z. Liu).

https://doi.org/10.1016/j.egyai.2021.100102
Received 22 May 2021; Received in revised form 12 July 2021; Accepted 16 July 2021
Available online 31 July 2021

Introduction

The transferring and storage of solar energy into hydrogen energy with a high energy density is a promising technology for accessing a renewable energy source. In addition, CO_2 utilization has been an important globe issue because CO_2 is the final stable oxidation product of fossil fuel utilization. Although CO_2 can be reduced to valuable products by additional energy input [1], energy requirements associated with the conversion of CO_2 to fuels is still one of the main issues in order to make an economically and environmentally sustainable process because the conversion of CO_2 to fuels should be made from a non-fossil resource [2]. The energy of solar radiation is just suitable in magnitude to induce transitions between electronic energy levels which can be harnessed as additional energy for the photocatalytic reduction of carbon dioxide [3, 4] to fuel production and photocatalytic splitting of water to hydrogen evolution [5, 6]. Utilizing CO_2 for the production of hydrogen by solar energy attract research due to the contribution of CO_2 reduction and hydrogen production. Although photoreduction of CO_2 to fuel and water splitting into hydrogen show great potential, the following challenges should be achieved for the practical utilization: (1) Composite semiconductor with available band gaps and p-n heterojunction; (2) Widen the absorbing range of solar spectrum and inhibit the reverse competition reaction; (3) Multi-electrons requirement for photoreaction by concentrated solar energy; (4) Lack of the detail mechanism in thermodynamic and kinetic; (5) Real efficiency under practical sunlight.

From the view of composite semiconductors, TiO_2 has been considered as a promising photocatalytic material for achieving the reduction of carbon dioxide and splitting of water for hydrogen evolution with solar energy due to its suitable band gap, sufficient band potentials and high charge transfer efficiency. Suitable modifications of TiO_2 improve the optical and electronic properties, including low visible light harvesting, hole-electron separation efficiency and reverse reaction in photoreaction process. Composite semiconductors, doping metals or non-metals, have been confirmed to enhance the optical properties. Composite semiconductors coupled the position bands of semiconductors have led to the benefit for the extension of visible light. $CdSe/TiO_2$ [7], CeO_2/TiO_2 [8], CdS/TiO_2 and Bi_2S_3/TiO_2 [9] were capable of enhancing the visible light absorption and photocatalytic activity of TiO_2. Although heterojunction formation prolongs the lifetime of charge carriers and prevents the recombination of electrons and holes, it is still necessary to find appropriate semiconductor pairs to reduce the recombination of charges with suitable composite band gaps.

Doping with transition metals on TiO_2 have been investigated to improve the photocatalytic activities. Doping with copper [10-12], silver [13-16], platinum [16, 17], palladium [18, 19] (18,19) and ruthenium [20] have been investigated to enhance visible light absorption and photocatalytic activity of TiO_2. The dopant loading level plays a key role in photocatalytic activity as the doping level could enhance the red shift towards visible light [21], while doping at high concentrations would result in the metal ions becoming recombination centres [22]. It was founded that Pt-doping with 0.5 wt% on TiO_2-ZnO can achieve maximum hydrogen yield 2150 mmolh-1g-1 enhanced at most 10% of water splitting into hydrogen [23] and Cu_2O are beneficial for CO_2 photoreduction [24]. Non-metals doping could also enhance the hydrogen production and CO_2 photoreduction [25].

TiO_2 particles display higher photocatalytic activities than TiO_2 films. However, one of the major drawbacks of TiO_2 particles is the costly photocatalyst separation that limits their practical application. Therefore, magnetic photocatalytic systems have been developed to enable easy recovery of the photocatalysts by an external magnetic trap [26, 27]. Researchers have prepared particles with a magnetic core and photoactive shell using magnetic granules and titania [28-30]. They have demonstrated that the composite particles exhibited magnetic properties and could be separated from a solution mixture by a magnetic field. However, researchers obtained different results on positive and negative photocatalytic activities. Some studies have reported the considerable reduction in photocatalytic oxidation activities in environmental purification schemes, especially in wastewater treatment. This negative behavior has been attributed to the injection of charges from TiO_2 into γ-Fe_2O_3 that induces photo-dissolution processes [28, 31] and subsequently led to reduced oxidizing power of the photogenerated holes. However, it is less reported the change of the reduction power of the photogenerated electrons has been less reported. Photocatalysts with photo-induced defect formation have been reported to improve photocatalytic reduction reactions [32].

Besides possessing magnetic properties, Fe_3O_4 is also a type of semiconductor. Fe_3O_4 coupling with TiO_2 could be a proper composite semiconductor for enhancing the charge separation due to the heterojunction, and the wider light absorption because of the presence of more conduction band and valance band positions. The available p-n heterojunction between Fe_3O_4 and TiO_2 is the key point to improve the activities of composite photocatalysts.

It is difficult to compare the activities of photocatalysts reported by different groups by only considering the conversion rate or quantum efficiency due to the differences of particular test conditions. Even though the photocatalysts are suitable for CO_2 reduction or H_2 evolution, the photocatalytic thermodynamics and kinetics are very important to enhance the efficiency of photoreaction. Some research works have been conducted to advance the light harvesting technique and improve the yield related to the reactor design and configuration [33, 34], temperature [35, 36], pressure [37] and pH of the solvent [38, 39]. However, few researchers discussed the results from the thermodynamics and kinetics aspects.

From the thermodynamics aspect, the potential of the electron acceptor (H_2O or CO_2 derivative) should be lower than the conduction band potential of TiO_2 and the driving force is the energy difference between the conduction band of TiO_2 and the reduction potential of the acceptor. Likewise, the potential of the electron donor should be higher than that of the TiO_2 valence band and the driving force is the energy difference between the valence band of TiO_2 and the oxidation potential of the donors. In view of this, TiO_2 photocatalysts are suitable for CO_2 reduction or H_2 evolution. Water splitting to hydrogen, and CO_2 reduction are both endothermal reactions, indicating the heat requirement and spontaneous reverse reactions.

Whereas in a kinetic aspect, electron–hole pairs excited by solar energy reduce CO_2 with H_2O depending upon the available activate electrons such as methane (CH_4) with 8 electrons, methanol (CH_3OH) with 6 electrons, formaldehyde (HCHO) with 4 electrons, carbon monoxide (CO) with 2 electrons and formic acid (HCOOH) with 2 electrons, while water reduction is a 2 electrons process. Electrons accumulation on the surface of photocatalysts would play an important role in multi-electron reaction.

It is reported that concentrated solar energy systems have an advantage for thermochemical applications because they can have more excited electrons with heat to drive endothermic chemical reactions [40]. Accordingly, concentrated solar energy systems could be beneficial for multi-electrons photoreaction due to more excited electrons evolution at the surface of photocatalysts.

In order to achieve the challenges, concentrated solar energy system was utilized to improve the CO_2 reduction for satisfying the heat requirement and multi-electrons photoreaction. Composite semiconductor with the available p-n heterojunction could improve the absorption ability. To afford a simplified and low-cost system, highly efficient photocatalysts TiO_2/Fe_3O_4, Cu_2O/TiO_2, $Cu_2O/TiO_2/Fe_3O_4$, $Pt/TiO_2/Fe_3O_4$ and Pt/TiO_2 were prepared and investigated towards the photoreduction of CO_2 and production of hydrogen in a practical concentrated solar energy system. In previous study [41], it demonstrated that products from CO_2 photoreduction, acting as sacrificial electron donors, improved hydrogen evolution in solar-mediated water splitting for prohibiting reverse reactions. Combining the amplification of photocatalytic activity with photocatalysts separation property,

magnetic features and composite semiconductors characteristics of photocatalysts present a promising technology for hydrogen evolution with improving solar energy absorption and multi-electrons CO_2 photoreduction under concentrated solar energy system condition.

2. Experimental and methodology

2.1. Composite semiconductor photocatalysts and characterization

Magnetic Fe_3O_4 core: Polyethyleneglycol (35.5 g) dissolved and dispersed in distilled water (15 mL) by sonication. After mixing with distilled water (40 mL), $FeCl_2$ (33 mL, 1%) andH_2O_2 (12 mL, 0.06 %) was added dropwise and the pH was adjusted within the range of 12 –13 using NaOH (3 M). The resulting solution was stirred at 55°C. After 2 h, the particles were separated by vacuum filtration and washed with deionized water until a neutral solution was achieved. The resulting filter cake was dried in air and thoroughly ground.

TiO_2/ Fe_3O_4: Tetrabutyl titanate (10 g) as Ti precursor was mixed with cyclohexanol (50mL) under stirring. Cetyl trimethylammonium bromide (CTAB) (0.04 g) as surfactant was dissolved in distilled water (20 mL). The above two solutions were mixed to obtain a yellow sol, which was stirred for 18 h. After that, the resulting sol was spread out to the prepared Fe_3O_4 particles with various amounts (i.e. 50 mg, 100 mg, and 150 mg). After adjusting the pH to 8.5, using triethanolamine and stirring for 4 h, a grayish-black sol formed that was centrifuged at 5000 rpm and subsequently washed with acetone thrice. The retrieved particles were dried in air and calcined at 500°C for 2 h.

Pt/TiO_2 and $Pt/TiO_2/Fe_3O_4$:TiO_2 (or TiO_2/Fe_3O_4) particles dispersed in an aqueous methanol solution (1 % by vol.) and then added $PtCl_2$ according to the ratio of 0.5 with Pt: TiO_2 (or TiO_2/Fe_3O_4). The resulting solution was sonicated for 20 mins and then heated to 75°C. After 1 h stirring, the suspension was irradiated at an Hg lamp under sonication for 20 h to deposit Pt nanoparticles onto the surface of TiO_2 (or TiO_2/ Fe_3O_4). After that, the powder was collected by filtration, washed twice with distilled water and then heated to 200°C for 2 h to remove any residual methanol.

Cu_2O/TiO_2 and Cu_2O/TiO_2/ Fe_3O_4: TiO_2 (or TiO_2/Fe_3O_4) particles dispersed in Cu $(NO_3)_2$ solution and then sonicated for 1 h. Subsequently, the resulting solution was heated to 95°C and was stirred further for 4 hrs. After filtration, the powder was heated to 150°C at a rate of 3°C/min for 2 hrs.

The prepared photocatalysts were characterized by X-ray diffraction (XRD) to analyse the crystal structure. A Philips X-PERT Pro Alpha 1 diffractometer was operated at a tube current of 40 mA and voltage of 45 kV with Cu Kα radiation ($\lambda = 1.5406$ Å). Data of 2θ was collected over a range of 20°–80° at a speed of 1°/min. Laser Raman spectra were investigated using Raman spectrometer (Perkin–Elmer Raman Station 400). The X-coordinate was calibrated using a silicon standard and the sharp Raman shifts are accurate within the limits of the resolution. Diffuse reflectance UV–vis spectra were collected by a UV–vis spectrophotometer (U-3310) equipped with an integrating sphere.

2.2. Activity measurements

2.2.1. Photocatalytic activity

Photocatalysts powder (TiO_2, TiO_2/Fe_3O_4 (1:1), TiO_2/Fe_3O_4 (1:2), TiO_2/Fe_3O_4 (1:3), Cu_2O/TiO_2, $Cu_2O/TiO_2/Fe_3O_4$ (1:2), 50 mg) for CO_2 reduction was dispersed in 100ml of distilled deionised water containing Na_2CO_3 (0.05%) and Na_2SO_3 (0.1%). After 10 mins sonication, hydrochloric acid was added to adjust the pH to 3. The resulting suspension in a quartz glass reactor (210ml) was then saturated by CO_2 with 30 mins bubbling. After that, the reactor was sealed and irradiated using a 250W Hg lamp with one sixth of the lamp irradiation. All reactors and lamp were immersed in a sonication tank with circulating water for cooling at ambient temperature. Hydrogen and methane in the gas, methanol, formic acid and formaldehyde concentrations in the liquid were detected by gas chromatograph (HP7890) while total organic carbon (TOC) concentration was investigated by TOC instrument (SHIMADZU TOC-VWP).

H_2 evolution photocatalysts (TiO_2, TiO_2/Fe_3O_4 (1:1), TiO_2/Fe_3O_4 (1:2), TiO_2/Fe_3O_4 (1:3), Pt/TiO_2 or $Pt/TiO_2/Fe_3O_4$ 50 mg) were dispersed in the filtered solution (100 ml) in a quartz glass reactor (210ml). The reactor was then thoroughly deoxygenated with argon and then sealed. After that, the suspension was irradiated using a 250W Hg lamp with one sixth of the lamp irradiation. The evolution of H_2 was measured by gas chromatography.

2.2.2. Photocatalytic activity at concentrated solar energy

Photocatalyst TiO_2/Fe_3O_4 powder (50 mg) mainly for CO_2 reduction was dispersed in distilled deionised water (100 ml containing 0.1% Na_2SO_3) with 10 mins sonication and then Pt/TiO_2 powders (50 mg) mainly for H_2 evolution was dispersed with a further 10 mins sonication. The suspension was adjusted at pH 3.0 by hydrochloric acid and then was bubbled with CO_2 for 30 mins in a quartz glass reactor (210ml). After sealing, the reactor was placed at the focus point of a dish-shaped solar collector under the practical sunlight. The solar collector was characterized with a concentration ratio of 17.6. The evolution of H_2 was measured by gas chromatography (HP7890) and TOC was measured by TOC instrument (SHIMADZU TOC-VWP).

2.3. AI Methodology

The Sobol sensitivity analysis was conducted the effects of Na_2SO_3 percentage, Na_2CO_3 percentage, pH value, ultraviolet, photocatalysts and total organic carbon and hydrogen production through MATLAB 2017a. Na_2SO_3 percentage, Na_2CO_3 percentage, pH value and ultraviolet are set as input and total organic carbon as output.

3. Results and discussion

3.1. Photocatalytic activities of hydrogen production and CO_2 reduction

In CO_2 photoreduction, excited electrons at more negative potential level can offer the driving force to reduce CO_2 for the expected chemical reaction. The concentration of dissolved CO_2 and derivative as well as pH are the main factors influencing the potential of half-reduction, which directly contribute to the selectivity and efficiency of the process. By comparing with the photoreduction potential at different pH values, the reduction potential moves to more negative potential level with the increase of pH, given in

The dominant ion of CO_2 and its derivatives vary with pH, where H_2CO_3 is the main existence ion at pH≤3.0 and CO32− species at pH≥10.3, while H_2CO_3 and HCO_3− are at 3.0≤pH≤6.3 [41]. Thus, the optimized pH for CO_2 photoreduction are in the range of pH≤3.0 or pH≥10.3 coupling with potential of CO_2 and derivative as well as TiO_2 conduction potential position, given in Fig. 2.

These results are in coincidence with CO_2 photoreduction at pH = 3 for the highest total organic content (TOC) [41] and at pH≥10.3 for maximum production of formic acid and formaldehyde with 0.15M NaOH [39]. From Fig. 2, the suitable pH range of TiO_2/Fe_3O_4 (1:2) is different from those of $Cu_2O/TiO_2/Fe_3O_4$ (1:2) and Cu_2O/TiO_2, the reason to be discussed in section 3.3.

In comparison with CO_2 reduction routes, [H+] is easier to be reduced into hydrogen in term of potential and the number of excited electrons. From the aspect of potential, the reduction potential of water to hydrogen is more positive than HCO_3 reduction to formic acid and formaldehyde except methanol. From the aspect of the number of excited electrons, [H+] reduction is a two electrons process while the CO_2 reduction is 4 - 8 electrons process to HCOOH, HCHO, CH_3OH and CH_4. The low solubility of CO_2 and derivatives in H_2O indicates that it is thermodynamically more favourable to reduce H_2O than CO_2 in the

competition of the CO_2 photoreduction process with hydrogen evolution.

The product desorption is the rate limiting step in the photosynthetic TOC by CO_2 reduction. The process includes light absorption, charge transport to photocatalyst surface, photoreaction with adsorbed reactants at the photocatalyst surface and photoproduct desorption from photocatalyst surface [41]. The TOC absorbed at the surface of photocatalysts, including HCOOH, HCHO and CH_3OH, may be further reduced to CH_4 by excited electrons instead of oxidation by holes if TOC did not consume quickly as a scarified agent in the hydrogen evolution process. The stirring of reactor was chosen to enhance the TOC desorption on the photocatalysts surface, and meanwhile co-catalyst has been chosen to conduct CO_2 photoreduction and hydrogen production, respectively.

The photocatalytic activities of the magnetic photocatalysts with different ratios, Pt-doping, Cu_2O doping photocatalysts and pure TiO_2 towards the photoreduction of CO_2 and photoproduction of hydrogen at the optimized conditions are given in **Table 1**.

The ranking of photocatalysts for the photoreduction of CO_2 is TiO_2/Fe_3O_4 (1:2) >TiO_2/Fe_3O_4 (1:3) >Cu_2O/TiO_2/Fe_3O_4 (1:2) >Cu_2O/TiO_2>TiO_2/Fe_3O_4 (1:1) >TiO_2. Whereas the ranking of photocatalysts for the H_2 evolution is Pt/TiO_2>TiO_2/Fe_3O_4 (1:2) > Pt/TiO_2/Fe_3O_4>TiO_2/ Fe_3O_4 (1:3) >TiO_2/ Fe_3O_4 (1:1) >TiO_2. TiO_2/Fe_3O_4 photocatalysts at varying Fe_3O_4 contents displayed higher efficiencies in comparison with pure TiO_2 for both the CO_2 photoreduction and hydrogen production processes. The TiO_2/Fe_3O_4 (1:2) photocatalysts showed a better performance than TiO_2/Fe_3O_4 (1:1) and TiO_2/Fe_3O_4 (1:3).

The heterojunction between TiO_2 and Fe_3O_4 ($FeO•Fe_2O_3$) may enhance the charge separation or increasing the probability of electron–hole recombination because all composite semiconductors performed higher activity than TiO_2, which had been investigated before [42]. Therefore, the structure and ratio of the TiO_2/Fe_3O_4 composite semiconductors play import roles on influencing the photocatalytic activities. The composite semiconductor was characterized with a wide-band gap TiO_2 semiconductor and a narrow-band gap of Fe_3O_4 ($FeO•Fe_2O_3$) semiconductor. The photogenerated electrons in the conduction band of TiO_2 tend spontaneously to transfer to the low-level conduction band of Fe_3O_4, FeO or Fe_2O_3 but reverse transferring by absorbing light, as shown in Fig. 1. Accordingly, the absorption range of solar spectrum enhanced by more existence of conduction bands. In addition, p-n heterojunction in composite semiconductor also conducts the improvement of photocatalytic activities due to the enhancement the separation of holes and electrons.

It is thermodynamically possible for the photogenerated holes to oxide the TOC to CO_2 because the valence band potentials of TiO_2, Fe_3O_4, FeO or Fe_2O_3 are more positive than the potential of TOC. The excited electrons at conduction bands cannot reduce CO_2 directly to CH_4, but could reduce CO_2 directly into TOC (HCOOH, HCHO, CH_3OH) in liquid phase, which result in a higher TOC.

Copper sites are considered to adsorb attractively CO_2 molecules, resulting in site activation. Moreover, Cu_2O is also a semiconductor like TiO_2, p-n heterojunction between the interface of Cu_2O and TiO_2 can serve to enhance charge separation and lead to suppress electron-hole pair recombination. Cu_2O/TiO_2/Fe_3O_4 (1:2) displayed a higher TOC by 1.5 times while Cu_2O/TiO_2 displayed a higher TOC by 1.33 times in comparison with the as-prepared TiO_2. As-prepared to Cu_2O/TiO_2/Fe_3O_4 (1:2) showed that doping Cu_2O on the surface of TiO_2/Fe_3O_4 (1:2) decreased the TOC formation relative to that of TiO_2/Fe_3O_4 (1:2). The possible mechanism is discussed in Section 3.3.

The XRD diffraction profiles of the as-prepared TiO_2 photocatalysts showed a well-crystallized anatase phase, while the as-prepared Fe_3O_4 particles could be indexed to the pure magnetite phase, as shown in Fig. 3. The TiO_2/Fe_3O_4 (1:2) photocatalyst also displayed the typical anatase peaks, as evident from the XRD pattern. This result indicated that small-sized Fe_3O_4 crystals in the composite sample were well integrated into the TiO_2 matrix. Two peaks, corresponding to the (311) and (440) planes of Fe_3O_4, were detected. This attributed to the possible dispersion of iron in the lattice of TiO_2. As the radius of an iron ion is similar to that of Ti^{4+}, substitution of iron in the matrix of TiO_2 is favourable.

The doping of Pt did not change the anatase phase of TiO_2. Although Cu_2O/TiO_2 particles did not influence the profile of the anatase phase, a broadened TiO_2 (004) plane peak was observed, which indicated the formation of amorphous layers on the particle surface.

Raman spectroscopy investigated the difference in the surface of the

Table. 1
Photocatalysts activities on hydrogen evolution and CO_2 photoreduction.

Photocatalysts	CO_2 photoreduction Hg lamp @250W pH =3, 50mg, 100ml,6h TOC, mg/L	TOC, mg/h.gcat	Hydrogen photoevolution Hg lamp @250W pH =3, 50mg, 100ml,6h H_2, umol/h.g	H_2, umol/h.g, TOC=183.5-190.8 mg/L
TiO_2	70.7	23.57	166.00	373.5
TiO_2/ Fe_3O_4 (1:1)	84	28.00	228.00	601.8
TiO_2/ Fe_3O_4 (1:2)	216.3	72.10	639.00	1538.1
TiO_2/ Fe_3O_4 (1:3)	117.6	39.20	290.50	677.9
Cu_2O/TiO_2	94.2	31.40	-	-
Cu_2O/TiO_2/ Fe_3O_4(1:2)	109.44	36.48	-	-
Pt/TiO_2	-	-	887.24	2001.2
Pt/TiO_2/Fe_3O_4	-	-	575.28	1305.7
	Concentrated solar energy pH =3, 50mg, 100ml,6h		Concentrated solar energy pH =3, 50mg, 100ml,6h	
TiO_2	66.3-70.7	22.1-23.6	166.0	373.5
TiO_2/ Fe_3O_4 (1:1)	78.8-84	26.3-28	228.3	601.8
TiO_2/ Fe_3O_4 (1:2)	131.3-140	43.8-46.7	339.0	788.6
TiO_2/ Fe_3O_4 (1:3)	110.3-117.6	36.8-39.2	290.5	677.9
TiO_2/Fe_3O_4 (1:2)&Pt/TiO_2	180.8-192.8	60.3-64.3	4531.0	8612.3

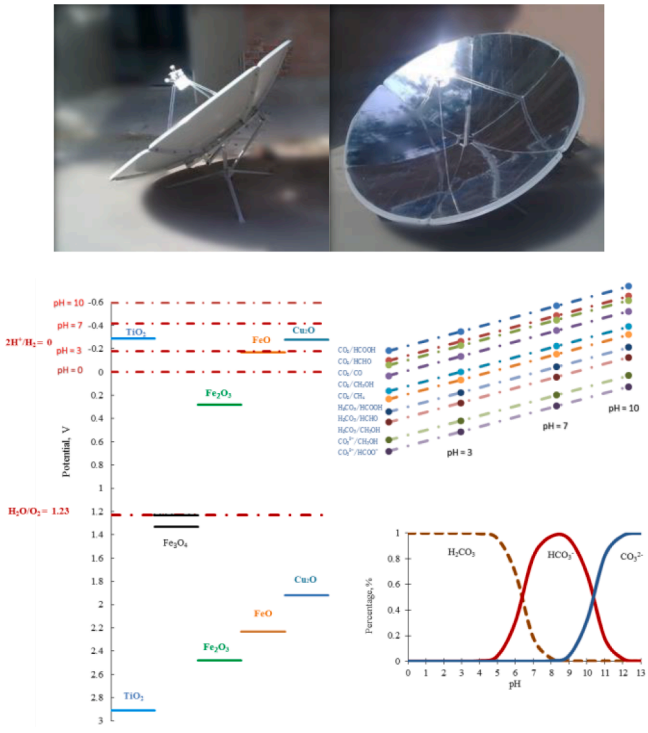

Fig. 1. The potential level of photocatalysts and thermodynamic potential versus pH for CO_2 photoreduction products and hydrogen evolution.

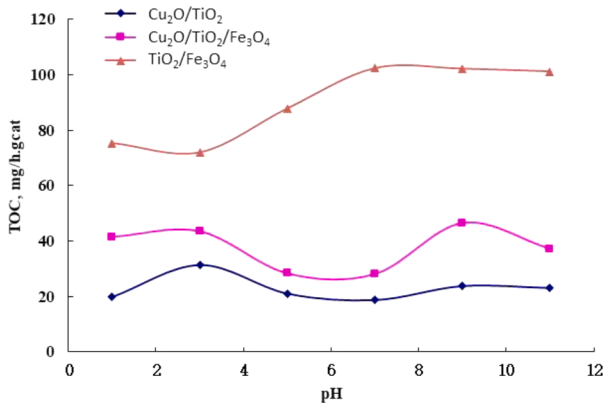

Fig. 2. pH effects on CO_2 photoreduction with photocatalysts.

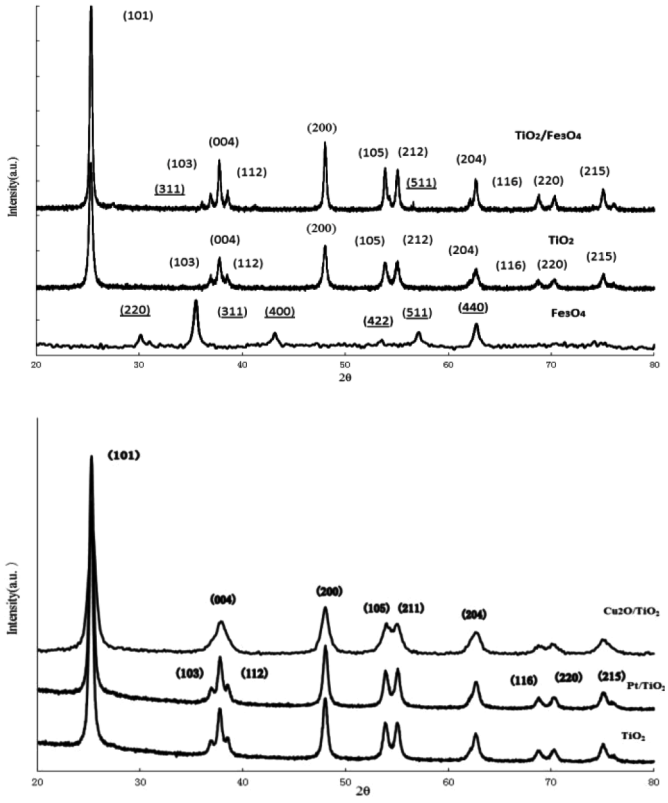

Fig. 3. XRD of as-prepared TiO_2 with (a) TiO_2/Fe_3O_4, Fe_3O_4 (b) Pt/TiO_2, Cu_2O/TiO_2.

crystalline structure. As TiO_2 anatase has a tetragonal structure with two formula units per unit cell, six Raman active modes have been observed according to group theory. In Fig. 4, the as-prepared TiO_2 photocatalysts displayed Raman active modes of anatase. The lowest frequency Eg mode at 143 cm−1 showed the strongest of all the observed peaks for anatase TiO_2 particles, which originated from the external vibration. Hence, the results indicated the existence of a long-range order structure. Raman spectrum of the as-prepared TiO_2/Fe_3O_4 particles also presents typical anatase features in spite of the lower intensity of the high-frequency Raman peaks. The absence of Raman features corresponding to crystalline Fe_3O_4 in the composite samples suggested that most of the Fe_3O_4 was embedded in the TiO_2 matrix. Pt/TiO_2 and Cu_2O/TiO_2 particles present a well-known anatase phase in Raman spectra with blue shift and line width shortening of the lowest frequency Eg mode and the intensity reducing of the high frequency Raman peaks. $Pt/TiO_2/Fe_3O_4$ also show an anatase phase with strongly reduction of the high frequency Raman peaks except of the lowest frequency Eg mode.

Based on UV–vis diffuse reflectance analysis (Fig. 5), both TiO_2 and TiO_2/Fe_3O_4 photocatalysts showed maximum absorption in the UV region. However, TiO_2/Fe_3O_4 photocatalyst that features a shoulder absorption peak in the visible spectral region suggested an enhanced visible light absorption.

The band gap of the photocatalysts can be calculated by the Kubelka–Munk theory [44, 45] and Tauc plots [46]. The linear region of the plots can be expressed as $(F(R)\bullet h\nu)n = K(h\nu - Eg)$ [47], where $h\nu$ denotes photon energy, Eg represents the band gap energy, n is either 1/2 or 2 and K is a constant that relates to the semiconductor material.

If a plot of $h\nu$ versus $(F(R)\bullet h\nu)2$ forms a straight line, a direct band gap can be observed by extrapolating the straight line to the $h\nu$ axis. Whereas, the measured band gap would infer an indirect transition when a plot of $h\nu$ versus $(F(R)\bullet h\nu)1/2$ forms a straight line. As observed from Fig. 5, a single band gap energy could be calculated for TiO_2, whereas two band gap energies were estimated for the TiO_2/Fe_3O_4 photocatalyst, as indicated by the extrapolation of the corresponding linear regions.

The calculated band gap energy of the as-prepared TiO_2 was 3.18 eV. Pt/TiO_2 and Cu_2O/TiO_2 were 3.15 eV and 2.98 eV. Two band gap values, corresponding to TiO_2/Fe_3O_4 (either Fe_2O_3 or FeO), could be estimated 2.95 eV and 2.2 eV, respectively. The band gap of Fe_3O_4 (0.1 eV) could not be detected by the current UV–vis spectrophotometer. The results confirmed that the TiO_2/Fe_3O_4 photocatalyst displayed enhanced visible light absorption that resulted in a higher photocatalytic activity when compared with that of pure TiO_2.

3.2. Thermodynamic and kinetic photocatalytic mechanism

3.3.1. P-n junction effects

Photocatalysts of TiO_2/Fe_3O_4 conducted to promote the photocatalytic activity both in CO_2 photoreduction to fuel and water splitting into hydrogen. The n-type TiO_2 semiconductor particle reacted with the Fe_3O_4 particle and concurrently produced p-type $FeTiO_3$ around the core of Fe_3O_4, thus solid p-n junction forms between p-type $FeTiO_3$ and n-type TiO_2 in the core-shell photocatalysts which enhance the isolation of holes with electrons with the help of the internal electric field of p-n junction, given in Fig. 6 (a). The similar enhancement also has been detected in p-type Cu_2O and n-type TiO_2, shown in Fig. 6 (b).

Pt-doping and Cu_2O doping change the internal electric field of p-n junction of TiO_2/Fe_3O_4 in different possible ways as shown in in Fig. 6 (c). The surface of $Cu_2O/TiO_2/Fe_3O_4$ presents the counterchange of negative charge and positive charge due to the p-n junction between Cu_2O and TiO_2 as well as the p-n junction between TiO_2 and Fe_3O_4. While TiO_2/Fe_3O_4 photocatalysts presents the accumulation of negative charge, which would result in the higher reduction activity than $Cu_2O/TiO_2/Fe_3O_4$. The mismatch resulted in enhanced charge recombination. Pt-doping may influence the internal electric field of p-n junction as the activity of $Pt/TiO_2/Fe_3O_4$ are lower than TiO_2/Fe_3O_4.

For comparing with the photocatalytic activities in visible light, the ratio of TOC concentration using TiO_2/Fe_3O_4 catalyst is 4.55 with Hg lamp as compared with Xe lamp, while the ratio of TOC concentration using Cu_2O/TiO_2 catalyst is 2.45, where the ratio of the number of photons is 5.0 times using 250W Hg lamp than 300W Xe lamp. TiO_2/Fe_3O_4 exhibited a 91% photocatalytic activity using Xe lamp and Cu_2O/TiO_2 presents a 49% at Xe lamp in CO_2 reduction in compared with Hg lamp. The results indicated the visible light absorption enhanced by TiO_2/Fe_3O_4 photocatalysts, which is in accordance with UV-vis diffuse detection results in Fig. 5.

3.3.2. Thermodynamic and kinetics mechanism

From the testing results of the photoreduction of CO_2 over TiO_2/Fe_3O_4 photocatalysts combined with hydrogenation of water splitting over Pt/TiO_2 under the concentrated sunlight, a possible reaction

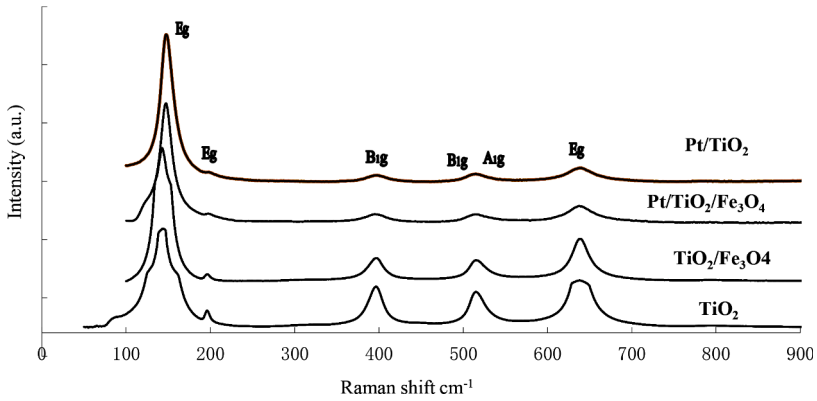

Fig. 4. Raman spectra of TiO_2, TiO_2/Fe_3O_4, Pt/TiO_2, $Pt/TiO_2/Fe_3O_4$.

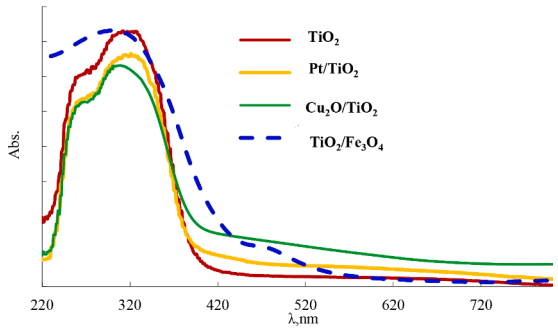

Fig. 5. Diffuse reflectance spectra of TiO_2, TiO_2/Fe_3O_4, Pt/TiO_2, Cu_2O/TiO_2.

pathway could be assumed. Firstly, incident photons are absorbed by photocatalysts and the photoexcited electrons move to the surface of TiO_2/Fe_3O_4 by internal electric field of p-n junction and the loaded Pt on Pt/TiO_2. Secondly, the electrons at the loaded Pt on Pt/TiO_2 reduce the water into hydrogen and CO_2 reduction proceeds competitively, while CO_2 tends to adsorb on Cu to reduce into CH_3OH, HCOOH and HCHO. Meanwhile, HCOOH, HCHO and CH_3OH can play the part of sacrificial agent on water splitting for improving hydrogen production.

In a thermodynamic aspect, CO_2 reduction is limited by its low solubility in water, the water reduction does not suffer from the similar problem, and thus the chance for electrons to meet and react with water is much higher than with CO_2. In a kinetic aspect, water reduction is a 2-electrons process, it is easier than most of the CO_2 reduction which required 4–8 electrons.

Combining the amplification of photocatalytic activity with photocatalysts separation property, magnetic features and composite semiconductors characteristics, photocatalysts present a promising technology for hydrogen evolution with improving solar energy absorption and multi-electrons CO_2 photoreduction under concentrated solar energy system condition. The study confirms the high efficiency (give the value) of the photoreduction of CO_2 over TiO_2/Fe_3O_4 photocatalysts combined with hydrogenation of water splitting over Pt/TiO2 (give the value) under concentrated sunlight.

3.3. AI analysis and concentrated solar energy effects

The results showed that CO_2 photoreduction at pH = 3 for the highest total organic content (TOC) with also highest hydrogen production. Based on the Sobol sensitivity analysis, the TOC concentration and hydrogen production could be influenced including the following parameters: Na_2SO_3 concentration, Na_2CO_3 concentration, pH and ultraviolet and visible light. According to the influence effects, the key parameters for TOC concentration were photocatalysts, Na_2CO_3 concentration and radiation intensity while the key parameters for hydrogen production were photocatalysts, radiation intensity, and TOC concentration.

The use of Pt doping on TiO_2 coupled with CO_2 photoreduction by TiO_2/Fe_3O_4 were investigated the concentrated solar energy systems. The Pt/TiO_2 photocatalyst decomposed water to produce H_2 and the TiO_2/Fe_3O_4 photocatalyst reduced CO_2 to organic compounds with TOC 183.5-190.8 mg/L and resulted in H_2 evolution 8343.5 – 8616.8 μmol/h. g. The reaction temperature significantly increased by concentrating solar irradiation and reached at 335K, which contributed to the acceleration both of hydrogen yield and CO_2 reduction.

The photocatalysts would reduce CO_2 into organic compounds with Na_2SO_3 as a sacrificial agent and decompose water to produce H_2 with TOC as a sacrificial agent. The presence of sacrificial reagents, acting as electron donors in water splitting, is crucial to prevent rapid hole-electron recombination and backward reaction. Pt doping on TiO_2 [43] has led to reduced exciton recombination, more efficient charge separation and reduced overpotential for hydrogen evolution. The photoreduction of CO_2 prefers more excited multi-electron at certain surface site of the particle. Photocatalysts are beneficial for providing more excited electrons at a time for achieving CO_2 photoreduction at the surface region of the particles with higher density of radiation by concentrated solar energy.

From a thermodynamic point of view, the formation of methane and methanol are more favorable in CO_2 reduction, since these reactions take place at lower potentials. However, the kinetic drawback makes methane and methanol formation more difficult than formaldehyde and formic acid because more electrons are required for the former reactions. Moreover, it is difficult to excite 2–8 electrons at a certain point

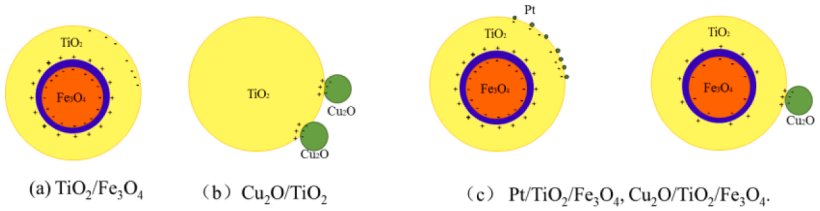

Fig. 6. The possible p-n junctions of photocatalysts.

to proceed with the CO_2 reduction. Due to the complicated nature of the inorganic photocatalysts surface, the interaction between photocatalysts and absorbed species tend to undergo a series of processes with less electron requirement instead of a multi-electrons process, and thus the actual reaction pathways are determined by redox potential required and available number of electrons.

Sufficient electron–hole pairs and available active photocatalytic points are the paramount factors for CO_2 photoreduction. Since CO_2 photoreduction is endothermal and CO_2 is a thermodynamically inert and very stable, the increase of temperature improves the efficiency by two aspects. One is to decrease the activated energy for photoreaction, and another is to enhance the transferring of charge carriers. This study indicated that concentrated sunlight is beneficial for a simultaneous supply of photons and thermal energy, which improve obviously the activity of photocatalysts.

4. Conclusions

The structure and content of the TiO_2/Fe_3O_4 composite semiconductors influence the photocatalytic activity. p-n junction formed favorably lead to the charge separation by internal electric field and otherwise the junction tends to serve as electron traps center by transferring photogenerated electrons to the low-level conduction band. Pt-doping and Cu_2O doping change the internal electric field of p-n junction of TiO_2/Fe_3O_4 in different ways. The surface of $Cu_2O/TiO_2/Fe_3O_4$ presents the cross field of negative charge and positive charge due to the PN junction between Cu_2O and TiO_2 as well as the PN junction between TiO_2 and Fe_3O_4, while TiO_2/Fe_3O_4 photocatalysts presents the accumulation of negative charge at the surface, which results in the higher reduction activity than $Cu_2O/TiO_2/Fe_3O_4$.

Sufficient amounts of electron–hole pairs and available active photocatalytic points are the paramount factors for CO_2 photoreduction because CO_2 photoreduction is endothermal and CO_2 is a thermodynamically inert and very stable compound. The concentrated sunlight is beneficial for a simultaneous supply of sufficient electron-hole pairs and thermal energy.

From a thermodynamic point of view, the formation of methane and methanol are more favorable in CO_2 reduction, since these reactions take place at lower potentials. However, the kinetic drawback makes methane and methanol formation more difficult than formaldehyde and formic acid because more electrons are required for the former reactions.

In thermodynamics aspect, water to hydrogen and CO_2 reduction are both endothermal reactions, which indicated the heat input requirement. CO_2 reduction is limited by its low solubility in water and thus the chance for electrons to meet and react with water is much higher than with CO_2. In a kinetic aspect, water reduction is a 2-electrons process, it is easier than most of the CO_2 reduction which required 4–8 electrons. Multi-electrons reaction can be achieved by concentrated sunlight.

The study confirms the high efficiency of the photoreduction of CO_2 over TiO_2/Fe_3O_4 photocatalysts combined with hydrogenation of water splitting over Pt/TiO_2 under concentrated sunlight.

Declaration of Competing Interest

The authors declare that they have no known competing financial interests or personal relationships that could have appeared to influence the work reported in this paper.

Acknowledgment

This paper was supported by Sino-Europe Research Program-China (MJ-2020-D-09)

References

[1] Guan GQ, Kida T, Yoshida A. Appl Catal B-Environ 2003;41:387–96.
[2] Keita I, Nozaki S, Ogawa M, Anpo M. Catal Today 2002;74:241–8.
[3] Teramura K, Tsuneoka H, Shishido T, Tanaka T. Chem Phys Lett 2008;467:191–4.
[4] Koci K, Obalova L, Matejova L, Placha D, Lacny Z, Jirkovsky J, Solcova O. Appl Catal B-Environ 2009;89:494–502.
[5] Lu HQ, Zhao JH, Li L, Gong LM, Zheng JF, Zhang LX, Wang ZJ, Zhang J, Zhu ZP. Energy Environ Sci 2011;4:3384–8.
[6] Hernandez-Alonso MD, Fresno F, Suarez S, Coronado JM. Energy Environ Sci 2009;2:1231–57.
[7] Wang CJ, Thompson RL, Baltrus J, Matranga C. J Phys Chem Lett 2010;1:48–53.
[8] Wang YG, Li B, Zhang CL, Cui LF, Kang SF, Li X, Zhou LH. Appl Catal B-Environ 2013;130:277–84.
[9] Li X, Liu HL, Luo DL, Li JT, Huang Y, Li HL, Fang YP, Xu YH, Zhu L. Chemical Engineering Journal 2012;180:151–8.
[10] Tseng IH, Wu JCS, Chou HY. J Catal 2004;221:432–40.
[11] Pinho LX, Azevedo J, Brito A, Santos A, Tamagnini P, Vilar VJP, Vasconcelos VM, Boaventura RAR. Chem Eng J 2015;268:144–52.
[12] Slamet HWNasution, Purnama E, Kosela S, Gunlazuardi J. Catal Commun 2005;6:313–9.
[13] Wu JCS. Catal Surv Asia 2009;13:30–40.
[14] Wu JCS, Wu TH, Chu TC, Huang HJ, Tsai DP. Top Catal 2008;47:131–6.
[15] Krejcikova S, Matejova L, Koci K, Obalova L, Matej Z, Capek L, Solcova O. Appl Catal B-Environ 2012;111:119–25.
[16] Zhang QH, Han WD, Hong YJ, Yu JG. Catal Today 2009;148:335–40.
[17] Wang Y, Lai QH, Zhang F, Shen XD, Fan MH, He YM, Ren SQ. RSC Adv 2014;4:44442–51.
[18] Ishitani O, Inoue C, Suzuki Y, Ibusuki T. J Photochem Photobiol A-Chem 1993;72:269–71.
[19] Xie TF, Wang DJ, Zhu LJ, Li TJ, Xu YJ. Mater Chem Phys 2001;70:103–6.
[20] Sasirekha N, Basha SJS, Shanthi K. Appl Catal B-Environ 2006;62:169–80.
[21] Anpo M. Pure Appl Chem 2000;72:1265–70.
[22] Gupta S, Tripathi M. Chin Sci Bull 2011;56:1639–57.
[23] Xie MY, Su KY, Peng XY, Wu RJ, Chavali M, Chang WC. J Taiwan Inst Chem Eng 2017;70:161–7.
[24] An XQ, Li KF, Tang JW. ChemSusChem 2014;7:1086–93.
[25] Guo SE, Tang YQ, Xie Y, Tian CG, Feng QM, Zhou W, Jiang BJ. Appl Catal B-Environ 2017;218:664–71.
[26] Xu SH, Shangguan WF, Yuan J, Chen MX, Shi JW. Appl Catal B-Environ 2007;71:177–84.
[27] Ao YH, Xu JJ, Zhang SH, Fu DG. J Phys Chem Solids 2009;70:1042–7.
[28] Chen F, Xie YD, Zhao JC, Lu GX. Chemosphere 2001;44:1159–68.
[29] Ma WF, Zhang Y, Li LL, You LJ, Zhang P, Zhang YT, Li JM, Yu M, Guo J, Lu HJ, Wang CC. ACS Nano 2012;6:3179–88.
[30] Chung YS, Park SB, Kang DW. Mater Chem Phys 2004;86:375–81.
[31] Beydoun D, Amal R, Low GKC, McEvoy S. J Phys Chem B 2000;104:4387–96.
[32] Yang XY, Salzmann C, Shi HH, Wang HZ, Green MLH, Xiao TC. J Phys Chem A 2008;112:10784–9.
[33] Nguyen TV, Wu JCS, Chiou CH. Catal Commun 2008;9:2073–6.
[34] Lee WH, Liao CH, Tsai MF, Huang CW, Wu JCS. Appl Catal B-Environ 2013;132:445–51.
[35] Wang ZY, Chou HC, Wu JCS, Tsai DP, Mul G. Appl Catal A-Gen 2010;380:172–7.
[36] Guan GQ, Kida T, Harada T, Isayama M, Yoshida A. Appl Catal A-Gen 2003;249:11–8.
[37] Kaneco S, Shimizu Y, Ohta K, Mizuno T. J Photochem Photobiol A-Chem 1998;115:223–6.
[38] Koci K, Obalova L, Placha D, Lacny Z. Collect Czech Chem Commun 2008;73:1192–204.
[39] Zhao ZH, Fan JM, Liu SH, Wang ZZ. Chemical Engineering Journal 2009;151:134–40.
[40] Yamashita H, Shiga A, Kawasaki S, Ichihashi Y, Ehara S, Anpo M. Energy Conv Manag 1995;36:617–20.
[41] Yang XY, Xiao TC, Edwards PP. Int J Hydrog Energy 2011;36:6546–52.
[42] Hsieh SH, Lee GJ, Chen CY, Chen JH, Ma SH, Horng TL, Chen KH, Wu JJ. J Nanosci Nanotechnol 2012;12:5930–6.
[43] Hakamizadeh M, Afshar S, Tadjarodi A, Khajavian R, Fadaie MR, Bozorgi B. Int J Hydrog Energy 2014;39:7262–9.
[44] Yang L, Kruse B. J Opt Soc Am A-Opt Image Sci Vis 2004;21:1933–41.
[45] Kubelka P. J Opt Soc Am 1948;38:448–57.
[46] T. J. Optical Properties of Solids 1969:123–36.
[47] Bhatt R, Bhaumik I, Ganesamoorthy S, Karnal AK, Swami MK, Patel HS, Gupta PK. Phys Status Solidi A-Appl Mat 2012;209:176–80.